NANO LETTERS

2008
Vol. 8, No. 5
1303-1308

Spatiotemporal Response of Living Cell Structures in *Dictyostelium discoideum* with Semiconductor Quantum Dots

Lam Helmick,[†,‡] Adriana Antúnez de Mayolo,[†,‡] Ying Zhang,[‡] Chao-Min Cheng,[‡] Simon C. Watkins,[§] Chuanyue Wu,[||] and Philip R. LeDuc*[,‡]

Departments of Mechanical and Biomedical Engineering and Biological Sciences, Carnegie Mellon University, 5000 Forbes Avenue, Pittsburgh, Pennsylvania 15213, Center for Biologic Imaging, S233 Biomedical Science Towers, 3500 Terrace Street, University of Pittsburgh, Pittsburgh, Pennsylvania 15261, and Department of Pathology, S-707B Scaife Hall, 3500 Terrace Street, University of Pittsburgh, Pittsburgh, Pennsylvania 15261

Received December 2, 2007; Revised Manuscript Received February 22, 2008

ABSTRACT

The ability to monitor the spatial and temporal organization of molecules such as biopolymers within a cell is essential to enable the ability to understand the complexity and dynamics existing in biological processes. However, many limitations currently exist in specifically labeling proteins in living cells. In our study, we incorporate nanometer-sized semiconductor quantum dots (QDs) into living cells for spatiotemporal protein imaging of actin polymers in *Dictyostelium discoideum* without the necessity of using complicating transmembrane transport approaches. We first demonstrate cytoplasmic distribution of QDs within these living amoebae cells and then show molecular targeting through actin filament labeling. Also, we have developed a microfluidic system to control and visualize the spatiotemporal response of the cellular environment during cell motility, which allows us to demonstrate specific localization control of the QD−protein complexes in living cells. This study provides a valuable tool for the specific targeting and analysis of proteins within *Dictyostelium* without the encumbrance of transmembrane assisted methods, which has implication in fields including polymer physics, material science, engineering, and biology.

Semiconductor quantum dots are inorganic nanocrystals that behave similar to fluorescent proteins yet have significant advantages over traditional molecular labeling methods. QDs represent a new class of labels for cellular imaging, which have significant advantages including their size scale and fluorescent properties.[1,2] QDs have a similar binding kinetic as conventional dyes, yet they do not exhibit a significant steric hindrance problem. Furthermore, the fluorescence emission of QDs is tunable by varying the particle size and composition; this allows for a narrow tunable spectra for emissions from multiple QDs to be resolved simultaneously without substantial spectral overlap.[3,4] The broad absorption bands make it possible to simultaneously excite multiple colors of QDs with a single excitation light source and to minimize sample autofluorescence by choosing an appropriate wavelength. Furthermore, QDs exhibit excellent photostability, which is critical in gathering data over extended time periods from single cell experiments. Photostability is a common limitation with conventional fluorescence approaches such as with green fluorescent proteins.[5,6] The large surface area of QDs also enables additional molecular interactions, which provide an advantage in a wide range of applications.[7–10]

Quantum dots have been of significant interest over the past decade in a diversity of applications at the molecular, cellular, and organism levels. QDs have the ability to be used as an inorganic system to visualize biological markers in both clinical and cellular studies. These nanoparticles have been used to study localization patterns in living animals for potential cancer detection[4] as well as labeling proteins in mammalian and plant cells.[11,12] QDs have also shown the potential to become a fluorescent label that would enable concurrent multiprotein analysis within a cell for long time imaging sequences. Labeling cellular structures within a cell often requires the transportation of the target cytoplasmic molecules across the cell membrane through additional molecular approaches. Studies have shown that QDs can enter the cytoplasm of specific cell types through actively controlled artificial transport methods which induce the cells to internalize the QDs.[11,12] This internalization though can

* Corresponding author. E-mail: prl@andrew.cmu.edu.
[†] Authors contributed equally.
[‡] Departments of Mechanical and Biomedical Engineering and Biological Sciences, Carnegie Mellon University.
[§] Center for Biologic Imaging, University of Pittsburgh.
[||] Department of Pathology, University of Pittsburgh.

10.1021/nl073144l CCC: $40.75
Published on Web 04/04/2008

result in the encapsulation of QDs limiting their ability to target specific cytoplasmic proteins. Jaiswal et al. demonstrated that after the endocytic uptake of QDs, the nanoparticles remained in a large number of vesicles 2−3 h after incubation.[13] While they remained in the vesicles though, the nanoparticles had no deleterious effects on cellular signaling or the motility of *D. discoideum* cells.

Visualizing time- and space-dependent processes in cells provides information that can be used to understand the complex dynamic behavior of cells. Cell motility is an essential biological process, which displays a coordinated set of spatial and temporal cues and responses to produce directed movement through structural organization of proteins including actin polymer filaments. In *Dictyostelium*, the cells actively move toward attractant molecules and require gradients of molecular responses such as polymerization to be initiated and maintained.[14] This process is critical in numerous physiological processes including wound healing, metastasis, immune response for mammalian cells, as well as cellular responses of keratinocytes, endothelial cells, and neurons.[15–17] Research shows that mammalian cells and *Dictyostelium*, although evolutionarily distinct, share similarities in molecular components and in response behaviors to chemical gradients.[18–20] This evolutionary conservation, combined with the accessible genetics and biochemistry of *Dictyostelium* cells, makes this free-living amoeba an important model to study the chemotactic pathway. Their movement can be controlled through chemical activation after starvation when *Dictyostelium* cells differentiate, polarize, and migrate in response to secreted cyclic adenosine 3′,5′-monophosphate (cAMP), which is mediated by cell surface cAMP receptors (cAR1−cAR4).[21,22] Previous analyses of *Dictyostelium* cells carrying the cAR1−GFP fusion construct have shown uniform protein distribution even after exposure to chemoattractant. However, even though cAR1−GFP does not redistribute in response to stimuli, this localized activation does result in a polarized response that induces localized actin polymerization, which requires spatial and temporal coordination.[14,23,24] Hence, developing a technique, which both controls the chemical input and then enables the visualization of these spatiotemporally coordinated events for actin filaments, would provide a platform technology for motility and cell structure.

Here, we utilize a combination of QDs and microfluidics to study the chemotaxis process of *Dictyostelium*. QDs are transported into the cell cytoplasm and then utilized to target actin filaments in these living cells. We also controlled the chemotactic response of the *Dictyostelium* using a microfluidics system. After creating a polarized cell response, we examined the localization of the QDs attached to actin polymers as biological markers with both time and space discrimination. Our results show the ability to target specific intracellular molecules in *Dictyostelium* using QDs without the use of artificial transmembrane transporter technology. This technique will enable a host of new studies to be undertaken without the complications of additional molecular internalization schemes. These studies also represent a combination of imaging and fabrication techniques and provide a valuable approach for studying the chemotactic response of *Dictyostelium* as well as demonstrating a new method that can be broadly applicable to live cell labeling.

A wild-type (Ax3) strain was grown at 22 °C to a cell density of 10^6 cells/mL in HL-5 media (per liter: 5 g of proteose peptone, 5 g of Thiotone E peptone, 10 g of glucose, 5 g of yeast extract, 0.35 g of $Na_2HPO_4 \cdot 7H_2O$, 0.35 g of KH_2PO_4). Cells were washed once and resuspended in fresh HL-5 medium or QD-containing HL-5 media. The QDs (Invitrogen; Qdot 605−Streptavidin #1010-1, Qdot 655−Phalloidin #1561-1) were incubated at a 10 nM final concentration (1:100 dilution) at room temperature. The QD_{605}−streptravidin was dissolved in HL5 media and sonicated for 10 min. Biotinylated phalloidin was mixed with QDs in a 1:10 ratio (with QDs at a 10 nM concentration). The QD_{605}−streptravidin−phallodin solution was incubated at room temperature for 30 min with mild stirring. At the end of the incubation time, the solution was centrifuged at 10000 rpm for 15 min to remove QD clusters. Cells were washed with Bonner's salt (per liter: 0.6 g of NaCl, 0.75 g of KCl, 0.3 g of $CaCl_2$) by three sequential centrifugations of 5 min at 5000 rpm. Cells were fixed by resuspension in 100% ice-cold acetone for 3 min. Cells were washed once with phosphate-buffered saline and stored at 4 °C until imaging. Cells were incubated with a 1:500 dilution of rhodamine phalloidin (Molecular Probes #R415) for 30 min at room temperature. *Dictyostelium* cells were placed on a glass slide and analyzed using an Olympus Fluoroview FV1000 microscope. Images were captured with an Olympus Fluoroview BX61 laser confocal microscope with a 100× plan apochromat objective at 1024 × 1024 pixel resolution and a magnification factor of 2× at the scan head. An argon−krypton laser produced excitation lines of 488 nm. The emission fluorescence wavelengths were restricted by a 505−550 nm bandpass filter. *Dictyostelium* cells were grown to 2×10^6 cells/mL concentration in HL5 media. The culture was plated on agar with Klebsiella bacteria for 2 days prior to motility experiment. Thereafter, cells were washed free of bacteria with Development Buffer (DB; 5 mM KH_2PO_4, 5 mM Na_2HPO_4, 2 mM $MgSO_4$, 0.2 mM $CaCl_2$), incubated for 1 h in DB buffer, and then pulsed with cAMP every 6 min for 4 h. Pulses of cAMP were added using a timer-controlled peristaltic pump, which was activated every 6 min for 10 s. Each pulse brought the solution to 100 nM cAMP concentration. At the end of the pulsing period, cells were washed once with PM buffer (5 mM Na_2HPO_4, 5 mM KH_2PO_4). Inverted channels were fabricated onto silicon wafers by pattern transferring with SU-8 photoresist. These are used to create microchannel molds. Poly(dimethylsiloxane) (PDMS) is cast against this mold and conformally seals against a borosilicate coverslide for microscopic visualization.[25,26] This microfluidics device controlled the gradient for directionally motility through equalizing the pressures at the inlet and outlet while adding cAMP to the opposite inlet relative to the *Dictyostelium*.

To study localized behavior of molecules within a living cell, QDs must first get across the cell membrane. We

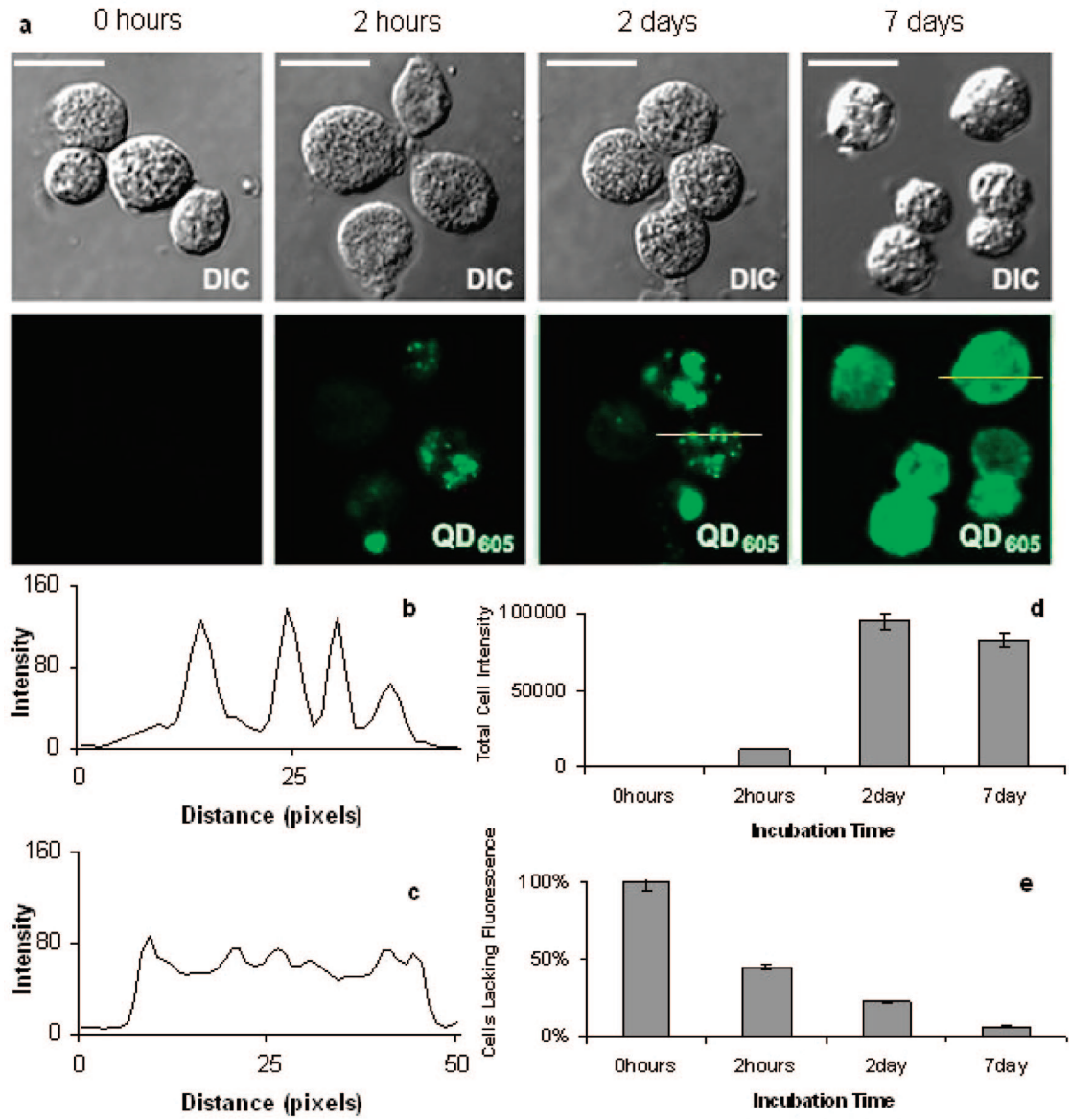

Figure 1. Understanding quantum dot (QD) distribution through controlling incubation time. (a) Differential interference contrast and fluorescent images with a fluorescein isothiocyanate filter of *Dictyostelium* containing QD-605. Line scan graphs for (b) 2 days and (c) 7 days to quantify the distribution and the intensity of QD fluorescence at each incubation period. Locations for the line scans are depicted as yellow lines in (a). (d) Fluorescence intensity in cells at each incubation time point. (e) Percentage of cells lacking fluorescence with respect to time. The scale bars are 10 μm.

accomplished this in *Dictyostelium* by incubating the cells with QDs and observing the distribution patterns over a controlled time course (Figure 1a). After a 2-h incubation, QDs were present as aggregates within the cell cytoplasm showing that transport was accomplished in a relatively short time frame. The *Dictyostelium* incorporated these nanometer scaled inorganic quantum dots into the cytoplasm, yet within this time frame these aggregates would likely not be able to target specific cytoplasmic molecules as they are not homogenously distributed in the cytoplasm (Figure 1a). This transport and pattern are likely due to the presence of vesicles that result from the endocytic uptake of QDs.[13] Following a 2-day incubation period, an increase in fluorescence intensity was observed revealing additional transport of QDs into the cytoplasm. However, the QD-labeled vesicles were still present (Figure 1a). When the incubation time was extended to 7 days, the fluorescence intensity distribution was observed to be more evenly distributed throughout the cytoplasm (Figure 1, panels b and c). This QD signal pattern is likely due to the release of the vesicular contents within the cell that occurs over time as the endocytic vesicles break down. We quantified the fluorescent intensity for each time point (Figure 1d), which revealed a pronounced increase in the amount of fluorescence per cell between the 2-h and 2-day samples. The fluorescent intensity though did not increase from 2 to 7 days suggesting a relative steady-state transport across the membrane of the QDs. In addition, the percentage of cells without fluorescence above background levels was calculated to quantify the success of QDs transport into the cells. The number of cells without QDs decreases with prolonged incubation time (Figure 1e) revealing that the efficiency of QD internalization increases over long time

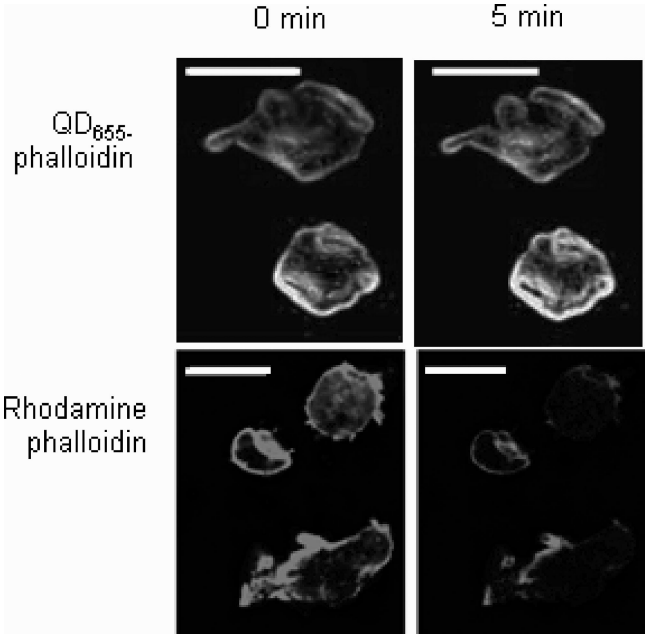

Figure 2. Fluorescent images of *Dictyostelium* with QD655−phalloidin and cells labeled with rhodamine phalloidin under a TRITC HYQ filter set, which is optimized for use with a tetramethylrhodamine isothiocyanate filter. After 5 min of fluorescent imaging, the photobleaching of the QD is minimal relative to the rhodamine phalloidin. Deconvolution and edge functions in NIH ImageJ were used for the images. The scale bars are 10 μm.

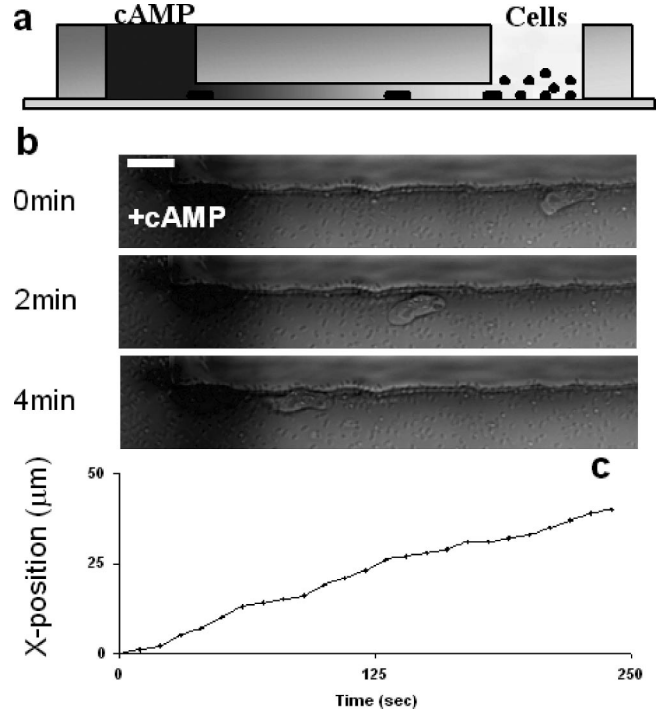

Figure 3. Controlling *Dictyostelium* chemotaxis. (a) A schematic of our approach for developing a controlled chemical gradient within our microfluidic channel. This induces cells to move toward the cAMP in the inlet well. (b) Sequential image of the motility response in a defined vector direction of a single *Dictyostelium* cell due to a controlled gradient of cAMP. The scale bar is 10 μm. (c) The movement of the cell with respect to time revealing the consistent directed motility of the cell toward the cAMP well; this was calculated through the position of the centroid of the cell.

periods. This transport effectiveness approaches 100% at these extended times indicating the effectiveness of this approach.

After establishing the ability of these cells to internalize the QDs into their cytoplasm, we wanted to specifically target proteins inside the cell. We focused on the actin cytoskeleton through labeling the polymerized form of actin with phalloidin. We first stained the *Dictyostelium* with phalloidin using conventional immunofluorescent staining techniques. These control cells were grown in HL-5 media lacking QD−phalloidin, fixed and permeablized, and then incubated with rhodamine phalloidin. These results were compared to labeling *Dictyostelium* with QDs conjugated with phalloidin through a 7-day incubation as described previously. The cells from both of the experiments were imaged to examine the spatial labeling of the actin filaments. Figure 2 shows cells separately labeled with either QD−phalloidin or rhodamine phalloidin. Both QD−phalloidin and QD are captured within vesicles at an early period and then released into the cytoplasm following vesicle release. The difference between them is that after release, QDs are homogeneously distributed throughout the cytoplasmic region, while QD−phalloidin will localize to actin filaments. In contrast to the cells in Figure 1a, which show QD_{605} homogeneously distributed through the cytoplasmic region at a later time period, QD−phalloidin-labeled cells show a specific pattern at a later time period, which is similar to the rhodamine phalloidin labeling experiments. This QD distribution in *Dictyostelium* suggests that the observed pattern corresponds to actin filaments. It is noted that the actin filament distribution for these experimental conditions in *Dictyostelium* is distinct from actin filament distribution observed in fully spread mammalian cells such as endothelial cells and fibroblasts where defined linear filaments are observed.[27] Also, there appears to be a slightly different distribution of the quantum dots between individual cells. This could be due to issues including variability from cell to cell or potentially some of the QDs being trapped in the vesicles. Furthermore, when QDs are compared to the conventional dye, our results also show the excellent photostability characteristics of QDs for our labeling. Our results demonstrated that the fluorescence intensity of rhodamine phalloidin diminishes after only minutes of fluorescence excitation, while there is minimal photobleaching with the QD−phalloidin.

After establishing the labeling approach for actin filaments in *Dictyostelium*, we wanted to probe the combined time and space distribution of the specifically targeted QDs during chemotaxis. Actin is known to have a high concentration at the leading edge of cells during chemotaxis, and we have demonstrated our ability to label actin polymers. Thus we next developed a technique to initiate local polarized response of *Dictyostelium* through inducing controlled cell motility. We dictated the response of *Dictyostelium* during motility with respect to time and space through stimulation using a microfluidics-based system. A chemical gradient was created using a two-inlet microfluidic channel made of PDMS (Figure 3a). Chemical cAMP at 100 μM was placed in the left inlet with the remainder of the channel and the right

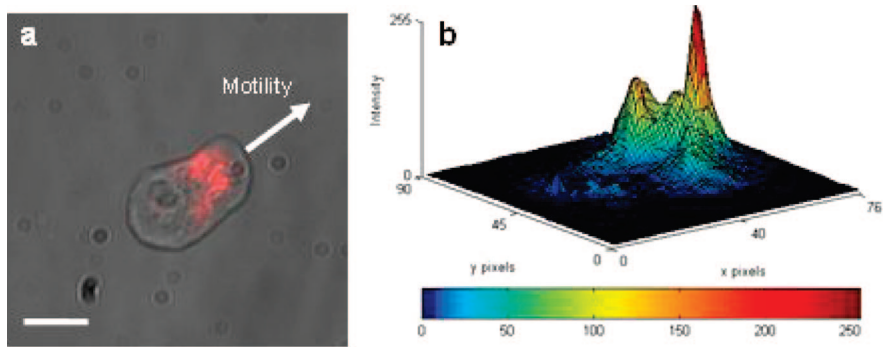

Figure 4. Localized response of phalloidin QDs in chemotactically responding *Dictyostelium*. (a) Composite differential interference contrast and fluorescent images (QD−phalloidin) of *Dictyostelium* moving in the direction of the arrow. (b) Surface plot of the intensity level (in the z direction) across the two-dimensional (x and y plane) in the fluorescent image showing the localization of the QDs at the leading edge of the cell. The absence of QDs is depicted in blue while the maximum intensity relating to the greatest presence of QDs is in red. The scale bar is 10 μm.

inlet only containing media. As there is limited flow in this system due to the equalization of the pressure, the cAMP diffused along the channel from the left inlet toward the right inlet creating a concentration gradient across the length of the channel. To visually verify that a gradient was established, Cascade Blue fluorescent dye was added to the cAMP solution, and although the diffusivity of these molecules was slightly different, the trends in the fluorescent response demonstrated our ability to create a controlled directional gradient using soluble molecules. Next, *Dictyostelium* cells were prepared for motility through pulsing with cAMP and then were pipetted into the right inlet. Directed motility was induced based on the gradient of cAMP as the cells moved along with channel toward the higher concentration of cAMP (Figure 3b; a movie of this motility is available as Supporting Information). The cell movement was quantified in terms of speed over the course of the experiment revealing a consistent velocity along the fluidic channel (Figure 3c).

After establishing the ability to control motility in *Dictyostelium*, we proceeded to investigate the response of cell structure during chemotaxis through our QD labeling approach of actin polymers. We used both QD_{655}−phalloidin as well as a surface modification strategy with QD_{605}−streptravidin conjugated with biotinylated phalloidin. The cells were incubated with QDs and then prepared for motility as previously described. During motility, QD fluorescence was observed to localize toward the leading edge of the cell (Figure 4a). Through examination of the intensity plot of the QD distribution within the cell, a highly compact region of fluorescence from the QDs was observed at the leading edge of the cells (Figure 4b). This was compared with the unactivated cells, which show a peripheral actin distribution throughout the cytoplasm of the phalloidin−QDs. As actin has been observed to be present in high concentrations at the leading edge of the cells, our results show the ability of this surface chemistry based modification strategy to succeed in exploring this polarized event; our data support the known findings on the reorganization of actin filaments to the leading edge during cell migration. Through the combination of QD and microfluidic technology, our approach has provided one method to obtain controlled input stimulation and spatiotemporal output for specific proteins in living cells.

Our ability to conduct space- and time-controlled studies on specific molecules in living cells without the necessity of complex intracellular targeting strategies will provide and exciting direction for a broad platform approach. Through our techniques, we have developed a system to study molecular responses associated with live *Dictyostelium* motility and to investigate polarized cell response. We have targeted specific proteins without the need of molecular transport catalysts. We also have implemented a microfluidics device that can create directed cell motility responses, which we used to examine the structural distribution in these cells. These studies will enable the ability to investigate a range of cellular processes and developmental biology questions that have remained unexplored in the past. This work will also allow for advances in multiple fields including simultaneous analysis of multiple chemotactic proteins to obtain real-time information as well as understanding structural organization in single living cells.

Acknowledgment. We thank the Dicty Stock Center for the kind donation of the strain used in this study, Jakob Franke and Kyle McQuade for help with *Dictyostelium* techniques, Stuart Shand and Jason Devlin for microscopy and QD support, and members of the LeDuc Laboratory. This work was also supported in part by the Department of Energy-Genome to Life, the National Science Foundation-CAREER, National Academies Keck Foundation Futures Initiative, Pennsylvania Infrastructure Technology Alliance, and the Beckman Young Investigators Program. C.W. would like to thank the NIH for support (GM65188).

Supporting Information Available: A video showing *Dictyostelium* cell motility. This material is available free of charge via the Internet at http://pubs.acs.org.

References

(1) Klarreich, E. *Nature* **2001**, *413*, 450–452.
(2) Mitchell, P. *Nat. Biotechnol.* **2001**, *19*, 1013–1017.
(3) Akerman, M. E.; Chan, W. C. W.; Laakkonen, P.; Bhatia, S. N.; Ruoslahti, E. *Proc. Natl. Acad. Sci. U.S.A.* **2002**, *99*, 12617–12621.
(4) Gao, X. H.; Yang, L. L.; Petros, J. A.; Marshal, F. F.; Simons, J. W.; Nie, S. M. *Curr. Opin. Biotechnol.* **2005**, *16*, 63–72.
(5) Bruchez, M.; Moronne, M.; Gin, P.; Weiss, S.; Alivisatos, A. P. *Science* **1998**, *281*, 2013–2016.
(6) Chan, W. C. W.; Nie, S. M. *Science* **1998**, *281*, 2016–2018.

(7) Dahan, M.; Levi, S.; Luccardini, C.; Rostaing, P.; Riveau, B.; Triller, A. *Science* **2003**, *302*, 442–445.
(8) Lidke, D. S.; Nagy, P.; Heintzmann, R.; Arndt-Jovin, D. J.; Post, J. N.; Grecco, H. E.; Jares-Erijman, E. A.; Jovin, T. M. *Nat. Biotechnol.* **2004**, *22*, 198–203.
(9) Medintz, I. L.; Clapp, A. R.; Mattoussi, H.; Goldman, E. R.; Fisher, B.; Mauro, J. M. *Nat. Mater.* **2003**, *2*, 630–638.
(10) Medintz, I. L.; Konnert, J. H.; Clapp, A. R.; Stanish, I.; Twigg, M. E.; Mattoussi, H.; Mauro, J. M.; Deschamps, J. R. *Proc. Natl. Acad. Sci. U.S.A.* **2004**, *101*, 9612–9617.
(11) Hanaki, K.; Momo, A.; Oku, T.; Komoto, A.; Maenosono, S.; Yamaguchi, Y.; Yamamoto, K. *Biochem. Biophys. Res. Commun.* **2003**, *302*, 496–501.
(12) Parak, W. J.; Boudreau, R.; Le Gros, M.; Gerion, D.; Zanchet, D.; Micheel, C. M.; Williams, S. C.; Alivisatos, A. P.; Larabell, C. *Adv. Mater.* **2002**, *14*, 882–885.
(13) Jaiswal, J. K.; Mattoussi, H.; Mauro, J. M.; Simon, S. M. *Nat. Biotechnol.* **2003**, *21*, 47–51.
(14) Parent, C. A.; Devreotes, P. N. *Science* **1999**, *284*, 765–70.
(15) Barak, L. S.; Ferguson, S. S. G.; Zhang, J.; Caron, M. G. *J. Biol. Chem.* **1997**, *272*, 27497–27500.
(16) Ferguson, K. M.; Lemmon, M. A.; Schlessinger, J.; Sigler, P. B. *Cell* **1994**, *79*, 199–209.
(17) Lemmon, M. A.; Ferguson, K. M.; Schlessinger, J. *Cell* **1996**, *85*, 621–624.
(18) Chen, M. Y.; Long, Y.; Devreotes, P. N. *Genes Dev.* **1997**, *11*, 3218–3231.
(19) Downey, G. P. *Curr. Opin. Immunol.* **1994**, *6*, 113–124.
(20) Parent, C. A.; Froehlich, W. M.; Devreotes, P. N. *Mol. Biol. Cell* **1998**, *9*, 383A–383A.
(21) Janssens, P. M. W.; Vanhaastert, P. J. M. *Microbiol. Rev.* **1987**, *51*, 396–418.
(22) Parent, C. A.; Devreotes, P. N. *Annu. Rev. Biochem.* **1996**, *65*, 411–440.
(23) Kreitmeier, M.; Gerisch, G.; Heizer, C.; Mullertaubenberger, A. *J. Cell Biol.* **1995**, *129*, 179–188.
(24) Gottwald, U.; Brokamp, R.; Karakesisoglou, I.; Schleicher, M.; Noegel, A. A. *Mol. Biol. Cell* **1996**, *7*, 261–272.
(25) Takayama, S.; Ostuni, E.; LeDuc, P.; Naruse, K.; Ingber, D. E.; Whitesides, G. M. *Nature* **2001**, *411*, 1016.
(26) Kuczenski, B.; LeDuc, P. R.; Messner, W. C. *Lab Chip* **2007**, *7*, 647–649.
(27) Cheng, C.-M.; LeDuc, P. R. *Adv. Mater.* **2008**, *20*, 953–958.

NL073144L